Triplet states in reaction center, light-harvesting complex B875 and its subunit form B820 from Rubrivivax gelatinosus observed by absorption-detected electron spin resonance in ze...

ARTICLE *in* BIOCHIMICA ET BIOPHYSICA ACTA (BBA) - BIOENERGETICS · OCTOBER 1995

Impact Factor: 5.35 · DOI: 10.1016/0005-2728(95)00099-5

ELSEVIER

Biochimica et Biophysica Acta 1231 (1995) 313–322

BBA Biochimica et Biophysica Acta

Triplet states in reaction center, light-harvesting complex B875 and its spectral form B840 from *Rubrivivax gelatinosus* investigated by absorbance-detected electron spin resonance in zero magnetic field (ADMR)

Vladimira Jirsakova [a,*], Françoise Reiss-Husson [a], Ileana Agalidis [a], Jacobine Vrieze [b], Arnold J. Hoff [b]

[a] *CGM, Bât. 24, CNRS, Av. de la Terrasse, 91198 Gif sur Yvette, France*

[b] *Department of Biophysics, Huygens Laboratory of the State University, P.O. Box 9504, 2300 RA Leiden, The Netherlands*

Received 4 November 1994; accepted 20 June 1995

Abstract

Absorbance-detected magnetic resonance (ADMR) spectroscopy was used for characterization of the triplet states in several pigment-protein complexes from *Rubrivivax gelatinosus*, namely the isolated reaction center, the core light-harvesting complex B875, and the B875 subunit form that absorbs in the infrared at 820 nm (B820), and, in the presence of glycerol, at about 840 nm (B840). The zero-field splitting parameters of the triplet states were determined and T − S spectra were recorded at 1.2 K. The absorbance and T − S spectra of the reaction center resemble closely those of *Rhodobacter sphaeroides*, except for slight shifts in the band positions. For the isolated B875 complex, only the triplet state of carotenoid was observed, indicating that triplet-triplet transfer from bacteriochlorophyll *a* to the carotenoid proceeds as in the native system. The near-infrared absorption spectrum of B840 at 1.2 K revealed several overlapping bands, which were deconvoluted in five Gaussian components corresponding to free BChl *a* (795 nm), B820 (826 nm), small population of B875 (888 nm) and two new spectral forms B846 and B868. The origin of these two latter spectral forms is proposed to reflect inaccurate reassociation of B820. Probably, oligomers of various sizes are formed, with different strengths of pigment-pigment and pigment-protein interactions. The T − S spectrum of B840 is consistent with that of a BChl *a* dimer containing a localized triplet state.

Keywords: ADMR; Photosynthesis; Purple bacterium; Antenna; Reaction center; Light-harvesting; (*R. gelatinosus*)

1. Introduction

Absorbance-detected magnetic resonance (ADMR) in zero magnetic field is a sensitive technique for investigating the triplet states of pigment-protein complexes. The ADMR technique correlates the optical and magnetic properties of a specific molecule and allows the assignment of zero-field splitting parameters to different triplet states. The method is particularly suited for the recording of the triplet-minus-singlet ground state (T − S) absorbance-difference spectrum [1].

The reaction center (RC) and light-harvesting complexes (LHC) are the basic units of the photosynthetic apparatus. The light-harvesting complex traps the light energy and transfers it to the RC. In RCs of purple bacteria, two separated charges are generated:

$$PBPhQ_A \xrightarrow[<10ps]{h\nu} P^+BPh^-Q_A \xrightarrow[200ps]{} P^+BPhQ_A^-$$

where: P is the primary donor (a BChl *a* dimer); BPh, a bacteriopheophytin; and Q_A a ubiquinone. When Q_A is chemically reduced before illumination, electron transport from BPh^- to Q_A is inhibited and the back reaction

$$P^+BPh^-Q_A^- \rightarrow P^TBPh^-Q_A^-$$

Abbreviations: P, primary donor; BPh, bacteriopheophytin; Q, ubiquinone; BChl, bacteriochlorophyll; RC, reaction center; LHC, light-harvesting complex; ADMR, absorbance-detected magnetic resonance in zero magnetic field; B875, core light-harvesting complex; B820 (B840), subunit form of core light-harvesting complex; $C_{10}E_4$, n-decyltetraoxyethylene.

* Fax: +33 1 69823562; e-mail: freiss@cgmvax.cgm.cnrs-gif.fr.

SSDI 0005-2728(95)00099-2

generates the triplet state of the primary donor (P^T) with a yield close to unity at cryogenic temperatures. Upon P^T formation, the RC has an absorption spectrum that is different from the singlet ground-state spectrum. The differences between the spectra can be measured by flash absorbance spectroscopy or by the several orders more sensitive ADMR spectroscopy. Triplet states can be formed also on isolated light-harvesting complexes by intersystem crossing following high intensity illumination. Generally, the amplitude of the ADMR signals for LHCs is much lower than for RCs, because of the much lower triplet yield for LHCs.

Besides the BChl and BPh chromophores, carotenoid pigments are present in wild-type RCs and light-harvesting complexes. Their function is on the one hand absorbing blue-green light and transferring the excitation energy to BChl molecules, on the other hand protection of BChl against harmful singlet oxygen formed by de-excitation of triplet BChl through triplet-singlet conversion with triplet O_2. Another role of carotenoids is the stabilization of LHC structure. Zurdo [2] showed that after extraction of carotenoids from LHC II of *Rhodobacter capsulatus*, the spectra of BChl were changed and also the stability of the protein decreased.

Carotenoid triplet states are very difficult to produce in vitro due to strong radiationless decay channels, which compete with the low intersystem crossing probability. The carotenoid triplet can be formed more easily when using triplet sensitizers whose lowest triplet level is nearly isoenergetic with that of the carotenoid triplet state. In photosynthetic systems, the natural triplet sensitizer is BChl and so the carotenoid triplet is formed by triplet-triplet transfer from ^{3}BChl to the carotenoid. Note that the energy of the carotenoid triplet is too low for forming singlet oxygen. The optical triplet-triplet absorption bands of carotenoids have been studied by flash-induced absorption spectroscopy [3] and magneto-optical difference spectroscopy [4]. The values of the zero-field splitting parameters were correlated to the number of conjugated double bonds in a carotenoid chain [5]. The assignment of the various bands in the T − S spectrum of RC and LHC of different species to carotenoids and BChl, has been discussed in a number of articles [6–12].

The core light-harvesting complex B875 (absorbing at room temperature at 875 nm) of various purple bacteria, e.g., *Rhodobacter sphaeroides* [13], *Rhodospirillum rubrum* [14], *Rhodopseudomonas marina* [15] and *Chromatium purpuratum* [16], can be dissociated into a small subunit form, B820, by the dissociating action of a detergent, either octyl glucoside (OG) or octyl dipropylsulfoxide (ODPS) [17]. Generally, this dissociation occurs in the absence of carotenoids. The subunit forms $(B820)_{OG}$ and $(B820)_{ODPS}$ can be again easily reconstituted to the original complex absorbing at 875 nm, even without addition of stabilizing carotenoids. Loach [18] even succeeded in reconstituting the B875 complex from the polypeptides α and β originating from different purple bacteria, and BChl *a*.

The B820 complex from *Rv. gelatinosus* was prepared from B875 by treating B875 with ammonium sulfate as described [19]. The treatment leads to partial conversion of large B875 oligomers to smaller oligomers (built from basic unit α/β:2BChl *a*:2 hydroxyspheroidene), shifting the main infrared maximum to 820 nm (B820). The behavior of B820 from *Rv. gelatinosus* differs in some aspects from other bacterial B820 forms. The specific carotenoid (hydroxyspheroidene) that is originally present in native antenna was shown to be required for correct reconstitution of the B875 complex from B820 [20]. If hydroxyspheroidene is not present, B820 at higher protein concentrations or in the presence of glycerol, or when ammonium sulfate is removed, is converted instead in a form absorbing at 840 nm at room temperature [19]. We note that glycerol was observed to stabilize the B875 form in *Rhodospirillum rubrum*; much more detergent was needed to cleave B875 to $(B820)_{OG}$ in its presence [21]. The B820–B840 transition does not modify the H-bonding pattern of the BChls: resonance Raman spectra of B840 from *Rv. gelatinosus* [22] are indeed similar to those measured for $(B820)_{OG}$ from *R. rubrum* [23].

The degree of oligomerization of B875 and B820 is still under discussion. Karrasch et al. [24] recently showed that in lipid bilayers 16 α/β subunits of *R. rubrum* form one B875 complex. Thermodynamic measurements of *R. rubrum* $(B820)_{OG}$ formation [25] indicate that it is a heterotetramer $[\alpha/\beta/2\ BChls]_2$, while spectroscopic properties of $(B820)_{OG}$ rather indicate an heterodimer $[\alpha/\beta/2BChls]$ [26,27]. In detergent solution, *Rv. gelatinosus* B875 is polydisperse, its smallest component being a dodecamer (Jirsakova, unpublished results) while B820 is a much smaller oligomer with apparent molecular weight about 20 kDa, probably just a heterodimer α/β with 2 BChl *a* and 2 hydroxyspheroidene molecules [19].

In this work, we applied ADMR spectroscopy to several pigment-protein complexes isolated from *Rubrivivax (Rv.) gelatinosus*: purified reaction centers, the core antenna B875 and the B840 complex. The spectroscopic properties of the RC triplet state are similar to those of *Rb. sphaeroides* RCs. ADMR and T − S spectra of the various antenna complexes are compared, giving clear evidence that the B840 complex is made up of a number of components, including B820, Car-containing B875 and at least two forms that presumably represent Car-free aggregates of B820. Upon triplet formation, the Car-free preparations show a bleaching and an appearing band at higher energy, indicating that at cryogenic temperatures B820 and its aggregates spectroscopically represent a BChl dimer.

2. Material and methods

Preparation of the samples. Reaction center, light-harvesting complex B875 and its subunit form B820 from

wild-type strain *Rv. gelatinosus* were prepared as described in [19,28,29]. Briefly, photosynthetic units composed of RC, B875, and tetraheme cyt *c* were isolated from the chromatophores by the detergent octyl thioglucoside (Fluka). Another detergent – $C_{10}E_4$ (Bachem) – was used for separating RC from B875 and cyt *c* by phase separation. The RC was further purified on a DEAE-Sepharose column and concentrated to an optical absorbance at 800 nm of 15 per cm. A small amount of tetraheme cyt *c* (about 1 cyt per 10 RC) was still present in the purified preparation. For ADMR measurements, the acceptor quinone Q_A was reduced by adding 30 mM sodium dithionite to RCs in a 50 mM Tris-HCl buffer (pH 8.0).

A mixture of B875 and of its subunit form, B820, was obtained by treating B875 with ammonium sulfate during hydrophobic chromatography. The two spectral forms of the core antenna were separated by gel filtration on an Aca 44 column. B875 was desalted from ammonium sulfate and both samples were concentrated to $A = 15$ per cm at the near-infrared maximum.

Glycerol was added to all samples (2:1, v/v) to prevent cracking upon cooling.

Carotenoid analysis in RC. TLC of RC pigments and spectroscopic identification were performed as described [19].

ADMR measurement. The principle of ADMR spectroscopy is described in detail elsewhere [11]. The samples (final optical absorbance at 800 nm about 0.5 per mm) in a cuvette with 1 mm pathlength were cooled slowly to 1.2 K in the dark and then illuminated with continuous white light of high intensity (about 2 W/cm^2) from a tungsten-halogen lamp. First, we recorded ADMR spectra by sweeping the microwave frequency at a fixed detection wavelength (chosen to correspond to an absorption band of carotenoid or BChl *a*). The amplitude of the microwaves was modulated at 312 Hz, and the resultant modulation of the transmitted light intensity detected phase-sensitively with a lock-in amplifier. Then, we chose a convenient microwave frequency and we recorded T − S spectra by variation of the detection wavelength. In the latter experiment, the microwaves were frequency modulated over the ADMR resonance for improving the signal-to-noise ratio.

3. Results and discussion

3.1. RC low-temperature absorption spectrum and carotenoid content

In Fig. 1, the low-temperature spectrum of *Rv. gelatinosus* RCs is shown. The 881 nm band originates from the photoactive dimer of BChl *a*, the 799 nm band from the two BChl *a* monomers, and the 759 and 749 nm bands are the Q_y transitions from photo-active and non-photo-active BPh, respectively. The 596 nm band arises from the Q_x transition of BChl *a* and the 546 nm band from the Q_x

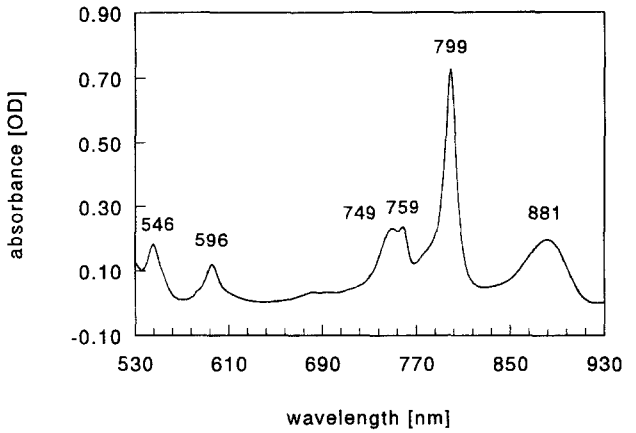

Fig. 1. Low-temperature (1.2 K) absorbance spectrum of *Rv. gelatinosus* RCs.

transition of the active BPh [11]. In the visible range, absorption bands due to carotenoids are observed [28]. Using thin-layer chromatography of pigment extracts, only one carotenoid species was detected; the absorption spectrum of the eluted carotenoid identified it as *spirilloxanthin*.

3.2. Low-temperature absorption spectra of B875 and B840

Fig. 2 shows the 1.2 K absorbance spectra of core antenna B875 and its aggregated subunit form B840. The near-infrared maximum Q_y of B875 is sharpened and shifted to 891 nm at low temperature. The band shape is asymmetric and has been explained by inhomogeneous broadening where each BChl has its own absorption whose maximum is influenced by the microenvironment of the protein matrix [30–33]. A Gaussian deconvolution (not shown) does not reveal any component of lower energy that would confirm the presence of the minor, strongly red-shifted spectral form proposed by Borisov et al. [34].

The B840 form has a very broad and complex low-temperature spectrum (Fig. 2B). We reported in [19] that when B820 was concentrated to high optical absorbance ($A > 10$ per cm) or when glycerol was added, its main absorbance maximum shifted to 835–840 nm and broadened at room temperature. At low temperature, the 840 nm band was shifted further to 845 nm and the broadening originated clearly from several absorption bands. Gaussian deconvolution revealed five bands in the B840 spectrum (Fig. 2B). Table 1 gives the maxima, half-widths and relative amplitudes of these Gaussian components. The broadest band with maximum at 795 nm is probably due to disconnected BChl *a*. The weak band of lowest energy, peaking at 888 nm, corresponds to residual B875. When the spectrum of B875 was substracted from the B840 spectrum, with a weight corresponding to the Gaussian 888 nm component, deconvolution of the difference spectrum revealed four bands with similar positions of maxima and relative ampli-

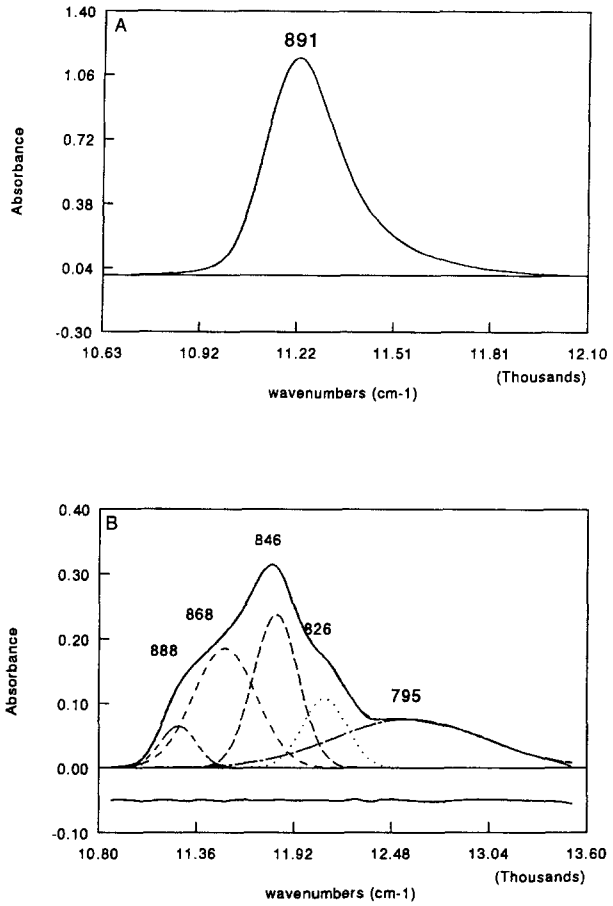

Fig. 2. Absorbance of B875 (A) and B840 (B) pigment-protein complexes at 1.2 K with deconvolution into Gaussian bands. The residual curve is shown below the spectrum and the characteristics of the bands are given in Table 1.

tudes as in the best fit obtained above (not shown). The 826 nm band can be ascribed to B820. The remaining major components, absorbing at 846 and 868 nm, apparently represent two distinct aggregation forms of B820.

Table 1
Principal bands from Gaussian deconvolution of absorption spectra (at 1.2 K) of B840

Wavelength (nm)	Width (nm)	Amplitude (rel.)
888	18	0.06
868	32	0.18
846	21	0.24
825	20	0.10
796	62	0.08

3.3. ADMR microwave spectra and zero-field splitting parameters

The zero-field splitting parameters |D| and |E| of BChl *a* and carotenoid triplets were determined by scanning the microwave frequency at several fixed detection wavelengths. Fig. 3A shows the strongest zero-field resonances of P^T: the |D| − |E| and |D| + |E| resonances are centered at 485 MHz and 658 MHz, respectively. Fig. 3B shows that the position, shape and width of the ADMR resonances depend on the detection wavelength as earlier observed for chromatophores of purple bacteria and RCs of Photosystem II of plants [12,33,35]. The 2|E| transition of the primary donor triplet of RCs was not detectable, most probably because of equal steady-state population of the *x* and *y* triplet sublevels. The observed transition frequencies and the zfs parameters are summarized in Table 2. The |D| and |E| values for P^T in RCs of *Rv. gelatinosus* are close to those found for P^T in other species [1,11].

We did not observe a RC carotenoid triplet transition when choosing as detection wavelength 585 or 570 nm, where the spirilloxanthin triplet absorbs. This absence of a carotenoid triplet in RCs agrees with results of Lous et al. [4], who measured triplet transfer from BChl *a* to carotenoid at different temperatures for RCs of *R. rubrum* and *Rb. sphaeroides* (wild type). At 1.2 K this transfer

Table 2
The zero-field splitting parameters of pigments from RC, B875 and B840 of *Rv. gelatinosus*

	2|E| (MHz)	|D| − |E| (MHz)	|D| + |E| (MHz)	|D| (10^{-4} cm^{-1})	|E| (10^{-4} cm^{-1})
RC					
BChl *a*	(173)	485	658	190.5	28.8
Spirilloxanthin	–	–	–	–	–
B875					
BChl *a*	–	–	–	–	–
Hydroxyspheroidene	211	(864)	1075	322	35.2
B840					
BChl *a*	(371)	474	845	219.6	61.8
	(383)	480	864	224.2	63.8
Hydroxyspheroidene	211				

The values in brackets were calculated, not measured.

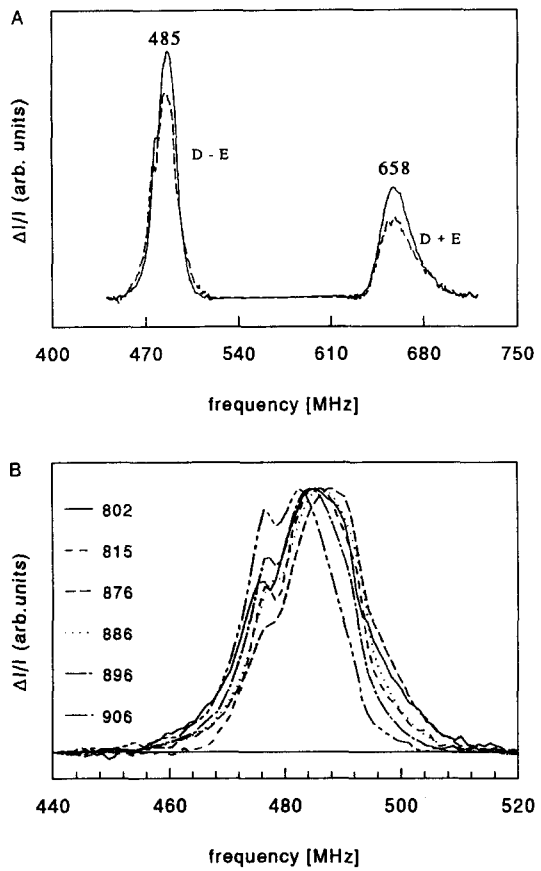

Fig. 3. (A) ADMR spectrum of the primary donor triplet state of RCs from *Rv. gelatinosus*, monitored at 890 nm (—) and 802 nm (– – –). (B) |D|-|E| transition of the primary donor triplet state from *Rv. gelatinosus* detected at different wavelengths (indicated at the left side of the spectra). The spectra are normalized at the band maximum.

does not occur because the activation energy then is too high. Lous et al. [4] found that the optimum of triplet formation was at 140 K. Aust et al. [5] reported parameters of the carotenoid triplet state measured at 20 K in a RC-B875 unit from *Rv. gelatinosus*, which were assigned to two carotenoid species. The minor species corresponded to a carotenoid with 13 conjugated double bonds, which agrees with spirilloxanthin.

Fig. 4A shows the ADMR microwave spectra of B875 and B840 with detection wavelength chosen at the carotenoid triplet absorbance, 530 nm. The strongest transition of hydroxyspheroidene is the 2|E| transition at 211 MHz. Although the signal amplitudes of the B875 and B840 complexes cannot be compared directly because of somewhat different experimental conditions; we estimate that the carotenoid triplet concentration in B840 was less that 20% of that of B875. Presumably, these carotenoid triplet in B840 originate from a small amount of residual B875 (Fig. 2B). We detected also the very weak |D| + |E| transition of the B875 carotenoid triplet at 1075 MHz (inset of Fig. 4A). No |D| − |E| transition could be observed, which is not surprising, as this transition is generally the weakest of the carotenoid resonances [5,10].

At a wavelength where possible BChl *a* triplet formation in B875 could be detected (891 nm), we did not observe a resonance (not shown). We conclude that virtually all triplets formed on BChl *a* in B875 were transferred to carotenoids; this indicates that the molecular configuration of the BChl-carotenoid complex is not modified by the isolation procedure.

In contrast, the microwave spectrum of B840 with detection wavelengths at 870, 844 and 822 nm (Fig. 4B) showed clearly, especially at the |D| + |E| BChl *a* frequency, two different triplet transitions between 845–850 MHz and 857–868 MHz, with maxima slightly shifted when detected at different wavelengths. The |D| − |E| transitions of the two triplets (at about 480 MHz) are more difficult to distinguish, the maxima also shifting with different detection wavelengths. The triplet signals overlapped considerably, even by selection of three different detection wavelengths we could not assign the triplet transitions to different absorption species.

Table 2 collects all observed triplet transitions and their zero-field splitting parameters |D| and |E|. The zfs parameter values that we found for hydroxyspheroidene are very close to the values published by Aust et al. [5] for the

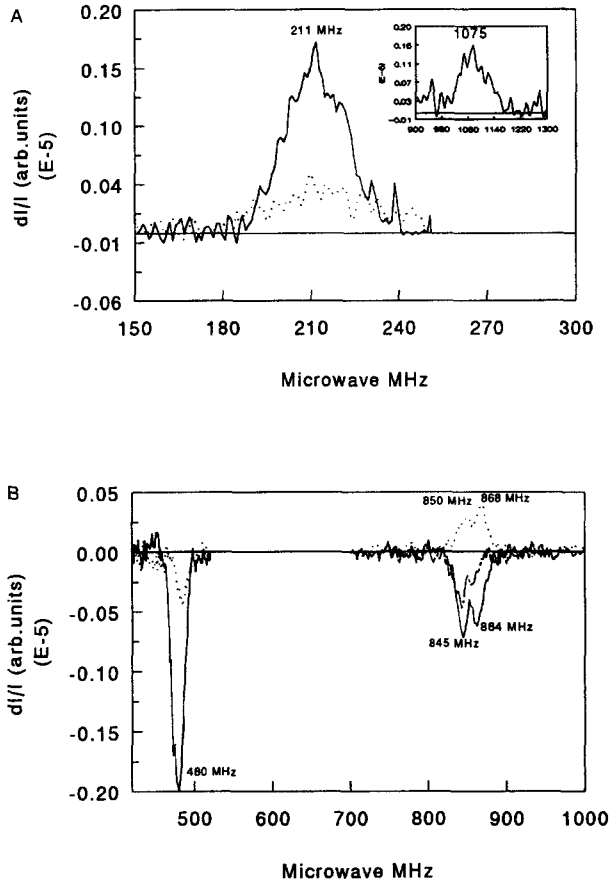

Fig. 4. ADMR spectra of (A) B875 (—) and B840 (· · ·), detected at 530 nm, and (B) B840, detected at 822 nm (· · ·), 844 nm (—) and 870 nm (– · –).

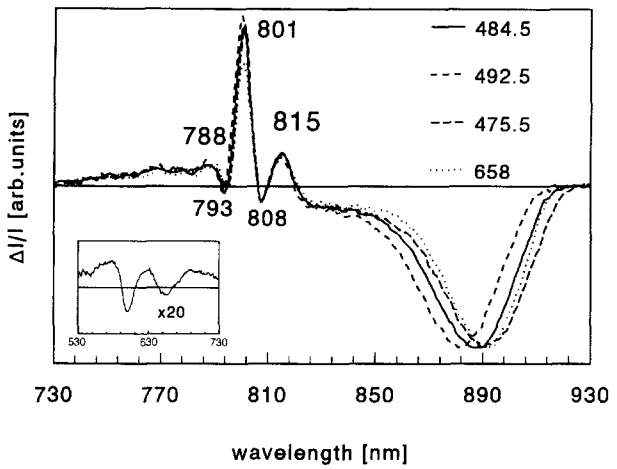

Fig. 5. T − S spectrum of the RC primary donor from *Rv. gelatinosus* between 730 and 930 nm, detected at various frequencies (resonance frequencies indicated in the right upper corner). The spectra are normalized at the 890 nm band. Inset shows the T − S spectrum between 530 and 730 nm (20× enlarged) recorded at the 484.5 MHz.

major carotenoid found in a B875-RC unit from *Rv. gelatinosus*, which had 10 conjugated double bonds.

3.4. Triplet-minus-singlet spectra

Reaction centers. Fig. 5 presents a T − S spectrum of the reaction center monitored at different transitions of the primary donor. We observe a large negative band around 880 nm originating from the bleaching of the Q_y absorbance of the primary donor. This band is inhomogeneously broadened and its position varies with the microwave frequency. Such variations have been explained by site effects; a site being defined as an environment of the pigments which gives rise to a particular set of zero-field splitting parameters. The amplitude of the Q_x bleaching at 601 nm (see inset of Fig. 5) is much weaker, probably because it overlaps with triplet-triplet absorption and positive bands of the accessory BChls.

Large oscillations appeared between 793 and 820 nm with maxima at 801 and 815 nm and a small minimum at 808 nm. These values are shifted compared to those of other bacterial species [11,36]; they are relatively insensitive to the microwave frequency. In the 740–790 nm region we observed a broad, featureless band, probably due to a slightly shifted absorption of BPh [11].

We have parameterized the changes in the 790–820 nm region of the T − S spectrum by spectral deconvolution. First the ground-state absorption spectrum of Fig. 1A was deconvoluted with Gaussian bands, centered at 807–808, 797–799 and 790–791 nm (Fig. 6a), analogous to the deconvolution of the absorption spectrum of *Rb. sphaeroides* [37]. The small shoulder at 807 nm is much weaker than the 812 nm band in *Rb. sphaeroides* [38]. The 777 nm band corresponds probably to free BChl *a*. Then, keeping fixed the fit parameters of the deconvolution of the ground-state absorption, which represents the negative 'singlet' part of the T − S spectrum, the positive 'triplet' part was deconvoluted (Fig. 6b). The positive bands are centered at 812, 799 and 793 nm. Because the T − S spectrum of the isolated reaction center is slightly dependent on the microwave frequency, we varied the positions of the negative band slightly for an optimal fit, the parameters of which are collected in Table 3.

Den Blanken and Hoff [11] ascribed the appearance of strong narrow bands at 807 or 838 nm (RC of *Rb. sphaeroides* R-26 and *Rps. viridis*, respectively) to the absorption of a monomeric BChl from the dimeric primary donor, in which the original singlet-singlet interaction is broken by the formation of a triplet state in which the interaction is much weaker. The 815 nm band was assigned to a shift to lower energy of the absorption of an accessory BChl *a*. We find, however, that the changes in the 790–820 nm region upon P^T formation can be attributed to shifts to slightly lower energies of the 802 and 808 nm transitions, and a small increase of dipolar strength at shorter wavelength (Fig. 6b). This interpretation is basically the same as that of the T − S spectrum of *Rb.*

Table 3
Fit parameters of the deconvolution of the absorbance (A) and T − S spectrum (B) of Fig. 6 in Gaussian bands

A Peak (nm)	Amplitude (a.u.)	Width (nm) (fwhm)	**B** Peak (nm)	Amplitude (a.u.)	Width (nm) (fwhm)
735	0.49	27.0	747	0.07	13.9
749	0.83	13.9	759	0.04	11.5
759	0.89	11.5	771	0.14	17.8
777	0.70	18.1	791	1.09	12.5
791	0.97	12.5	793	−0.97	12.5
799	2.95	9.3	797	−2.95	9.2
807	0.63	11.7	799	4.16	9.2
826	0.25	81.9	807	−0.63	11.7
872	0.60	34.2	812	0.58	11.8
888	0.53	25.7	826	−0.15	81.9
			877	−0.57	34.6
			891	−0.55	25.8

sphaeroides [37]. For the latter species we found from the polarizations of the absorption bands in the T − S spectrum as determined by linear-dichroic ADMR, which do not change upon P^T formation, that the two positive bands in the 790–820 nm region at 818 and 808 nm, the analogues of the 812 and 799 nm bands in the T − S spectrum of *Rv. gelatinosus*, arise from band shifts to lower energies [37].

The general similarity between the T − S spectrum of *Rv. gelatinosus* and the T − S spectra of other purple bacteria [11,12] provides strong evidence that the structure of the primary donor and its immediate environment is quite similar for all species studied. This agrees with resonance Raman studies of *Rv. gelatinosus* RC [39], which indicated that the structural properties of the primary donor in its oxidized and reduced states are comparable to that of *Rb. sphaeroides*, particularly at the level of hydrogen bonding pattern of the conjugated carbonyls, and of the charge delocalization in the oxidized state.

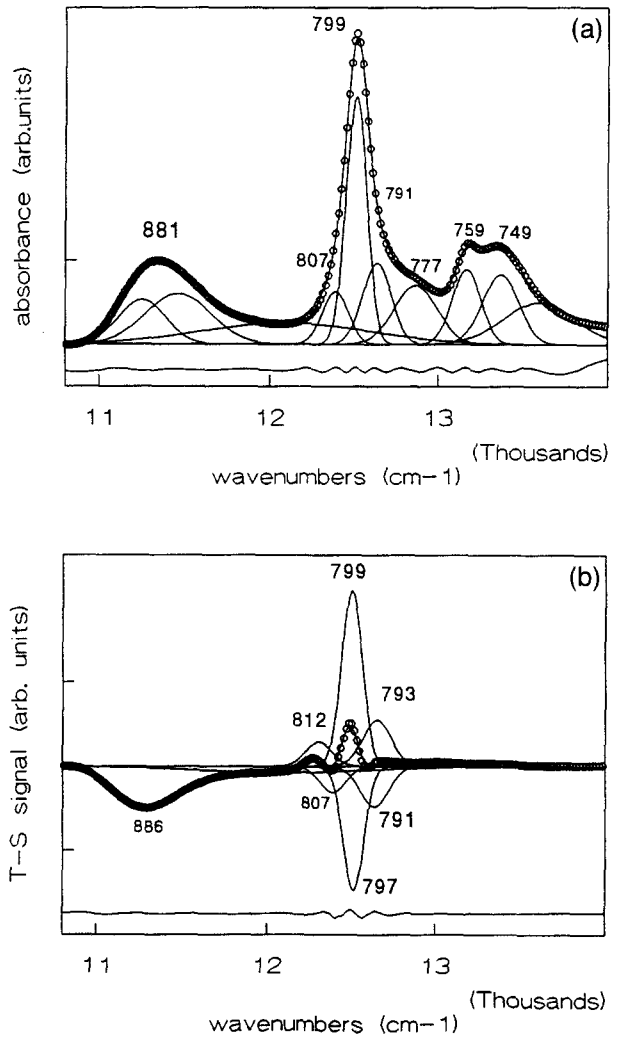

Fig. 6. Gaussian deconvolution of the low-temperature ground-state absorption (a) and T − S (b) spectra of RCs of *Rv. gelatinosus*. The negative part of the deconvolution of the T − S spectrum represents the ground-state absorption spectrum.

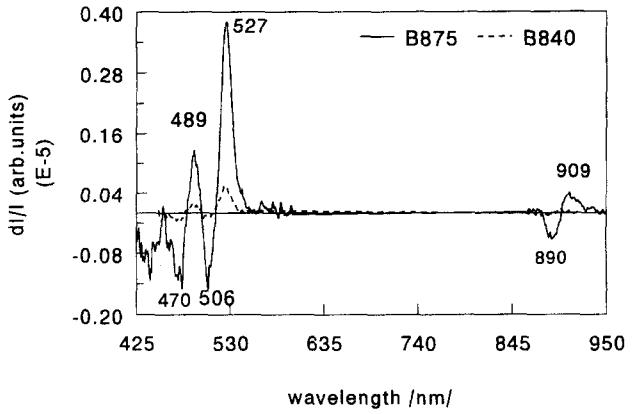

Fig. 7. T − S spectrum of B875 and B840 detected at 211 MHz.

B875 and B840 complexes. Fig. 7 compares T − S spectra of B875 and B840 from *Rv. gelatinosus* detected at the carotenoid 2|E| transition, at 211 MHz. By correlating ADMR microwave spectra with T − S spectra, it is possible to distinguish between different sets of carotenoid molecules within one given preparation [10]. We previously determined only one type of carotenoid in B875 (and B820); the T − S spectra in the carotenoid absorption region support this result. The positive bands at 527 and 489 nm originate from hydroxyspheroidene triplet-triplet absorption. The minima at 440, 470 and 506 nm correspond to hydroxyspheroidene singlet-singlet absorption, which in vivo at room temperature occurs at 440, 470 and 500 nm (data not shown).

In previous work [19] we suggested that the few carotenoids present in B820 (or B840) after isolation were distributed randomly, and were included in detergent-protein micelles. The microwave and T − S spectrum of B840 in the carotenoid region, however, shows that these carotenoids are still in a functionally active state, so that the BChl and Car are close enough and in native-like orientation to allow efficient triplet transfer from BChl to Car. During the purification it was not possible to deplete completely the Cars from B820. As the Cars have a strong affinity for the B820 complex and help to reform the native antenna [20], we suppose that Cars are implicated in a structural connection between neighboring B820 units.

In B875 we also observe absorbance changes in the BChl *a* near-infrared region when exciting the carotenoid triplets. These bands are due to a change in BChl *a* absorption induced by the presence of a carotenoid triplet [10]. The signal coming from B840 was too weak for being detected.

Fig. 8 presents T − S spectra of B840 in the BChl *a* region detected at different frequencies. The spectra recorded at the |D| − |E| transitions (Fig. 8a and Fig. 8b) had lower amplitudes and their shapes were rather differ-

ent from those taken at the |D| + |E| transitions (Fig. 8c and 8d). The different aspects of the T − S spectrum of B840 recorded at the two microwave transitions are caused by the presence of two triplet states with somewhat different zero-field parameters, whose microwave transitions strongly overlap (Fig. 4b). As a consequence, it is not possible to excite these triplets individually, and the T − S spectrum of B840 depends on the frequency of the exciting microwaves.

All four spectra were decomposed into Gaussian bands. Comparison between these bands (Fig. 8a–d) and the Gaussian bands from the B840 absorption spectrum (Fig. 2B) shows that the negative bands of the T − S spectra result from a bleaching of the absorption bands at 868, 846, 826 and 795 nm. No negative band at 888 nm is seen, which indicates that B875 is not bleached in the T − S spectrum of B840. Indeed, the triplets formed on the B875 BChls are transferred to Cars and are seen in the Cars spectra (Fig. 4A and 7). A positive band around 832 nm is observed in all four difference spectra and another weaker one around 790 nm. It is generally believed that, at least at cryogenic temperatures, the BChls in B875 are spectroscopically dimeric and that this global configuration is retained in the B820 form of the core antenna. Extending this hypothesis to B840, the shape of its T − S spectrum recorded at the more or less homogeneous transition is readily explained. When the triplet state is formed, the singlet-singlet interactions between the BChl molecules of the dimer are broken, and the absorption of the dimer in slightly different configurations (absorbing at 826, 846 and 868 nm, Table 1) is bleached. Assuming that the triplet state is localized on one BChl, the singlet ground-state absorption of the other dimer-half will arise at lower wavelength. The spectra of Fig. 8 indicate that the monomeric BChl *a* formed in both B846 and B868 absorbs at the same wavelength (832 nm). The area of the 832 band is about the half the sum of the areas of the B846 and B868 bleachings, seen most clearly in the two best fits (Fig. 8c and 8d) where the signal is less noisy. The monomeric BChl absorption coming from B826 appears at about 790 nm. Van Mourik et al. [26] measured the T − S spectra of $(B820)_{OG}$ from *R. rubrum* and found the posi-

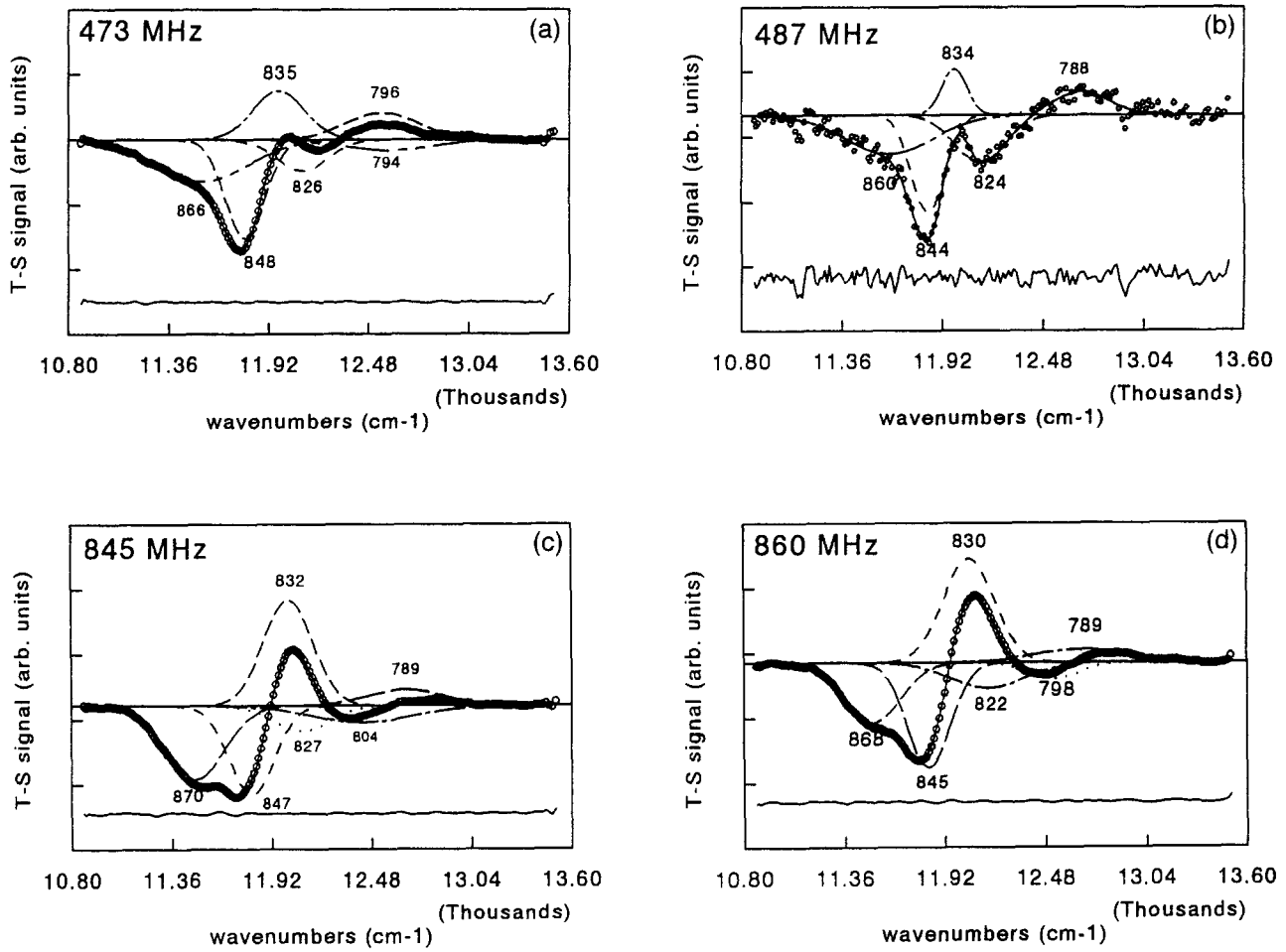

Fig. 8. T − S spectra of B840 detected at different triplet transitions (indicated at the left upper corners) and their Gaussian deconvolution with residual curves under the spectra.

tive monomer absorption band at about 800 nm. Apparently, the monomer absorption may be slightly influenced by the nature of the detergent.

One may note that a minor spectral form peaking at 845 nm has also been observed during reassociation of *Rb. sphaeroides* $(B820)_{ODPS}$ [17]. Because of its large bandwidth (fwhm = 51 nm), this component was proposed to be a ODPS-solubilized BChl dimer. In *Rv. gelatinosus* B840, the bandwidths of the 846 and 868 nm bands are similar to that of the 826 nm band, and we therefore conclude that they represent protein-bound BChl complexes. Indeed, Raman spectroscopy has shown [22] that BChl *a* in *Rv. gelatinosus* B840 presents an H-bond pattern of its conjugated carbonyls similar to that of, for example, *R. rubrum* $(B820)_{OG}$. Electron microscope images (Jirsakova, unpublished data) indicate that the particle size is larger in B840 than in B820. Ghosh et al. [40] has shown that B868 of *R. rubrum* constitutes elongated structures, presumably composed of aggregated $(B820)_{OG}$ units. Thus we believe that in the B846 and B868 spectral forms, the BChl *a* is present as a protein-bound dimer, whose absorption is influenced by 'incorrect' oligomerization of B820 in the absence of the required carotenoid. The spectral shifts probably originate both from excitonic interactions between BChl dimers placed close together and from the changes in protein microenvironment of the BChl dimer caused by aggregation.

Our spectroscopic data strongly suggest that at cryogenic temperatures the B820 and its aggregates B846 and B868 represent BChl dimers. For B875, this could not be checked because of the fast BChl-Car triplet transfer.

4. Conclusions

The spectral characteristics of the triplet state of the primary donor in *Rv. gelatinosus* RCs are similar to those observed for other purple bacteria [1,11]. The relative intensities of the zero-field transitions and the |D| values of P^T are comparable in magnitude. The general shape of the T − S spectrum of *Rv. gelatinosus* is basically the same as for other purple bacteria and can be interpreted in the same way, with only minor shifts in the positions of the absorption maxima of the accessory BChls to longer wavelength. Thus, the structure of the primary donor of *Rv. gelatinosus* and its environment resembles that of other purple bacteria.

The similarities between *Rv. gelatinosus* and *Rb. sphaeroides* RCs do not extend to the nature of their bound carotenoid, which is spirilloxanthin in the former (as shown here) and spheroidene in a 15–15′ *cis* conformation in the latter. This was unexpected, as spirilloxanthin is less abundant than spheroidene in *Rv. gelatinosus* chromatophores. The conformation of spirilloxanthin is still unknown and should be probed by other techniques, such as Raman spectroscopy.

Recently, interactions between pigments have been studied in purified light-harvesting complexes from photosynthetic organisms by ADMR [10]. Application of this technique to isolated B875 indicates that transfer of excitation energy from BChl to hydroxyspheroidene still occurs in the solubilized complex. The B840 form, which is formed from B820 at low temperature and in the presence of glycerol, displayed a much more complicated behavior. It still contained a small population of B875 generating a carotenoid triplet with 'native' characteristics. Its other spectral components were devoid of functional carotenoids and generated only BChl triplets. The T − S spectrum showed several components, indicative of antenna BChls in several slightly different (dimeric) configurations. Triplet formation generated an absorption at shorter wavelength, interpreted as the (monomeric) singlet ground-state absorption of one-half of a BChl dimer containing a localized triplet state. Thus, in the B840 form of *Rv. gelatinosus* Bchl *a* appears to be bound to the protein matrix as a dimer, as generally accepted for the B820 forms of the core antenna in other bacterial species.

Acknowledgements

We thank to Mrs. M.-C. Gonnet for the preparation of chromatophores from the culture of *Rv. gelatinosus*. This work has been supported by C.N.R.S. and a scholarship to V.J. from the French Government.

References

[1] Den Blanken, H.J. and Hoff, A.J. (1983) Chem. Phys. Lett. 98, 255–262.
[2] Zurdo, J., Fernandez-Cabrera, C. and Ramiez, J.M. (1993) Biochem. J. 290, 531–537.
[3] Monger, T.G., Cogdell, R.J. and Parson, W.W. (1976) Biochim. Biophys. Acta 449, 136.
[4] Lous, E.J. and Hoff, A.J. (1989) Biochim. Biophys. Acta 974, 88–103.
[5] Aust, V., Augerhofer, A., Ullrich, J., Von Schütz, J.V. and Wolf, H.C. (1991) Chem. Phys. Lett. 181, 213–221.
[6] Rockley, M.G., Windsor, M.W., Cogdell, R.J. and Parson, W.W. (1975) Proc. Natl. Acad. Sci. USA 72, 2251–2255.
[7] Holten, D., Windsor, M.W., Parson, W.W. and Thornber, J.P. (1978) Biochim. Biophys. Acta 501, 112–126.
[8] Shuvalov, V.A., Klevanik, A.V., Sharkov, A.V., Matveetz, Yu.A. and Krukov, P.G. (1978) FEBS Lett. 91, 135–139.
[9] Shuvalov, V.A. and Parson, W.W. (1981) Proc. Natl. Acad. Sci. USA 78, 957–961.
[10] Van der Vos, R., Carbonera, D. and Hoff, A.J. (1991) Appl. Magn. Res. 2, 179–209.
[11] Den Blanken, H.J. and Hoff, A.J. (1982) Biochim. Biophys. Acta 681, 365–374.
[12] Den Blanken, H.J., Van der Zwet, G.P. and Hoff, A.J. (1982) Chem. Phys. Lett. 85, 335–338.
[13] Chang, M.C., Meyer, L. and Loach, P.A. (1990) Photochem. Photobiol. 52, 873–881.
[14] Miller, J.F., Hinchigeri, S.B., Parkes-Loach, P.S., Callahan, P.M.,

Sprinkle, J.R., Riccobono, J.R. and Loach, P.A. (1987) Biochemistry 26, 5055–5062.
[15] Meckenstock, R.U., Brunisholz, R.A. and Zuber, H. (1992) FEBS Lett. 311, 128–134.
[16] Kerfeld, C.A., Yeates, T.O. and Thornber, J.P. (1994) Biochim. Biophys. Acta 1185, 193–202.
[17] Visschers, R.W., Nunn, R., Calkoen, F., Van Mourik, F., Hunter, C.N., Rice, D.W. and Van Grondelle, R. (1992) Biochim. Biophys. Acta 1100, 259–266.
[18] Loach, P.A., Parkes-Loach, P.S., Davis, C.M. and Heller, B.A. (1994) Photosynth. Res. 40, 231–245.
[19] Jirsakova, V. and Reiss-Husson, F. (1993) Biochim. Biophys. Acta 1183, 301–308.
[20] Jirsakova, V. and Reiss-Husson, F. (1994) FEBS Lett. 353, 151–154.
[21] Visschers, R.W., Chang, M.C., Van Mourik, F., Loach, P.A. and Van Grondelle, R. (1990) in Current Research in Photosynthesis (Baltscheffsky, M., ed.), Vol. II, pp. 133–136, Kluwer, Dordrecht.
[22] Jirsakova, V., Reiss-Husson, F., Robert, B. and Sturgis, J. (1994) Lithuanian J. Phys. 34, 344–347.
[23] Visschers, R.W., Van Grondelle, R. and Robert, B. (1993) Biochim. Biophys. Acta 1183, 369–373.
[24] Karrasch, S., Bullough, P.A. and Ghosh, R. (1995) EMBO J. 14, 631–638.
[25] Sturgis, J. and Robert, B. (1994) J. Mol. Biol. 238, 445–454.
[26] Van Mourik, F., Van der Oord, C.J.R., Visscher, K.J., Parkes-Loach, P.S., Loach, P.A., Visschers, R.W. and Van Grondelle, R. (1991) Biochim. Biophys. Acta 1059, 111–119.
[27] Visschers, R.W., Van Mourik, F., Monshouwer, R. and Van Grondelle, R. (1993) Biochim. Biophys. Acta 1141, 238–244.
[28] Agalidis, I. and Reiss-Husson, F. (1992) Biochim. Biophys. Acta 1098, 201–208.
[29] Agalidis, I. and Reiss-Husson, F. (1991) Biochem. Biophys. Res. Commun. 177, 1107–1112.
[30] Pullerits, T., Visscher, K.J., Hess, S., Sundström, V., Freiberg, A. and Van Grondelle (1994) Biophys. J. 66, 236–248.
[31] Timpmann, K., Freiberg, A. and Godik, V.I. (1991) Chem. Phys. Lett. 182, 617–622.
[32] Van Mourik, F., Visschers, R.W. and Van Grondelle, R. (1992) Chem. Phys. Lett. 193, 1–7.
[33] Reddy, N.R.S., Picorel, R. and Small, G.J. (1992) J. Phys. Chem. 96, 6458–6464.
[34] Borisov, A.Y., Gadonas, R.A., Danielius, R.V., Piskarskas, A.S. and Razjivin, A.P. (1982) FEBS Lett. 138, 25–28.
[35] Van der Vos, R., Van Leeuwen, P.J., Braun, P. and Hoff, A.J. (1992) Biochim. Biophys. Acta 1140, 184–198.
[36] Vasmel, H., Den Blanken, H.J., Dijkman, J.T., Hoff, A.J. and Amesz, J. (1984) Biochim. Biophys. Acta 767, 200–208.
[37] Vrieze, J. (1994) Doctoral Dissertation, Leiden.
[38] Feher, G. (1971) Photochem. Photobiol. 14, 373–387.
[39] Agalidis, I., Robert, B., Mattioli, T. and Reiss-Husson, F. (1992) in The Photosynthetic Bacterial Reaction Center II (Breton, J. and Verméglio, A., eds.), Plenum Press, New York, pp. 133–139.
[40] Ghosh, R., Kessi, J., Hauser, H., Wehrli, E. and Bachofen, R. (1990) in Molecular biology of membrane-bound complexes in phototrophic bacteria (Drews, G. and Dawes, E.A., eds.), pp. 245–251, Plenum, New York.